1Pb2-5

3-D FDTD simulation of moving sound source and receiver with directivity

Takao Tsuchiya[1†], Yu Teshima, and Shizuko Hiryu[2] ([1]Faculty of Science and Engineering, Doshisha Univ., [2] Faculty of Life and Medical Science, Doshisha Univ.)

1. Introduction

Finite difference-time domain (FDTD) method [1] is a most popular numerical method for the sound field analysis. We have implemented moving sound sources and receivers for the FDTD method [2, 3]. However, in those analyses, the source and receiver were omnidirectional and the effect of the moving speed on the amplitude was not considered. In this paper, this scheme is extended to the moving source and receiver with directivity. Formulation and numerical experiments are carried out for the moving monopole, dipole, and the cardioid sources and receivers.

2. Theory

2.1 Implementation of moving source and receiver

To implement a moving sound source in the FDTD method, the grid points around the moving path of the sound source are driven with the following Gaussian distribution function.

$$f_s^n(i,j,k) = e^{-\alpha_s d_s^2} \quad (2)$$

where $f_s^n(i,j,k)$ is source distribution at the grid point $(i\Delta, j\Delta, k\Delta)$ at time $t = n\Delta t$, Δ is grid interval, Δt is time step, d_s is the distance between the center of the source and the driving grid point, and α_s is the source size parameter. In this paper, $\alpha_s = 0.7$, and the grid points within 3Δ of the distance from the center of source are simultaneously driven with the amplitude of $Q^n f_s^n(i,j,k)$ where Q^n is the source signal at $t = n\Delta t$.

In the case of a moving receiver, the basic idea is the same as that of a moving source. The sound pressure at the receiver is interpolated from the sound pressures at the surrounding grid points using the Gaussian function as

$$p_r^n = \sum_{i,j,k} e^{-\alpha_r d_r^2} p_{i,j,k}^n \quad (2)$$

where d_r is the distance between the center of the receiver and the grid point, and α_r (=0.7) is the receiver size aprameter, and $p_{i,j,k}^n$ is sound pressure at grid point (i,j,k) at time *n*.

2.1 Doppler effect

As shown in Fig. 1, it is assumed that a sound source moves with a velocity $\boldsymbol{v}_S$ and a receiver moves with a velocity $\boldsymbol{v}_R$. The Doppler shift is determined by the radial velocity v_{SR} for the sound

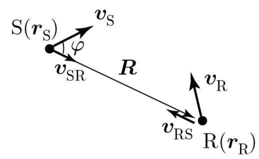

Fig.1 Positional relationship between moving sound source S and moving receiver R.

source and v_{RS} for the receiver given as

$$v_{SR} = \frac{\boldsymbol{R}_{RS}\cdot \boldsymbol{v}_S(t_S)}{R}, \quad v_{SR} = \frac{\boldsymbol{R}_{RS}\cdot \boldsymbol{v}_R(t_R)}{R} \quad (3)$$

where $\boldsymbol{r}_S$ is the source position vector evaluated at the sound radiation time, and $\boldsymbol{r}_R$ is the receiver one evaluated at the receiving time. So, the normalized Doppler shift *D* at the receiver R is given as

$$D = \frac{c_0 - v_{RS}}{c_0 - v_{SR}} \quad (4)$$

In the case of a moving monopole source, the fundamental solution is given as [4]

$$p_m = \frac{Q}{4\pi R(1-M_{SR})} e^{-jkR} \quad (5)$$

where $k = \omega/c_0$ wave number, ω is angular frequency of the source, $M_{SR} = v_{SR}/c_0$ is the radial Mach number of the monopole. For a moving dipole oriented in the *x*-direction, the sound pressure is given for $kR \gg 1$ as

$$p_x \approx \frac{-jk\cos\theta}{4\pi R(1-M_{SR})^2} e^{-jkR} \quad (6)$$

where θ is angle with *x*-axis. A cardioid consists of a monopole and a dipole in equal proportions, in which case the dipole signal must be time integrated.

3. Numerical experiments

Numerical experiments are performed by the CE-FDTD (IWB) method [5,6]. Figure 2 shows a 3-D numerical model for the directivity of the fixed source and receiver. The grid size is Δ=15 mm, time step is Δt=44.1 μs, and sound speed is $c_0 = 340$ m/s, so the Courant number χ is 0.99. The boundary condition is Mur's first order absorbing boundary. In the figure, Q is a receiver when P is a

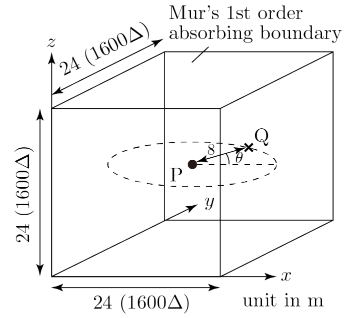

Fig.2 Numerical model of directivity analysis for fixed source or receiver.

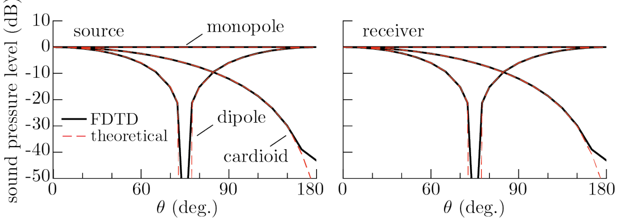

Fig.3 Directivity of fixed source and receiver.

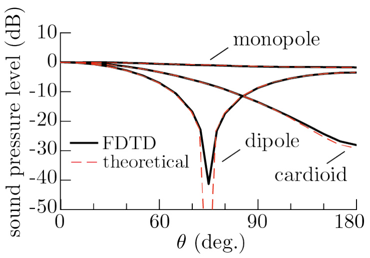

Fig.4 Directivity of moving source (M=0.1).

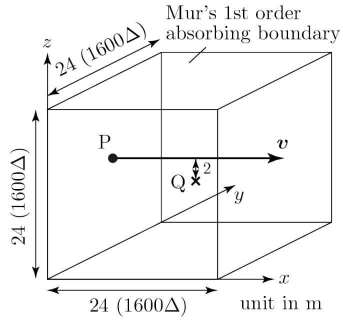

Fig.5 Numerical model for a linearly passing source or receiver.

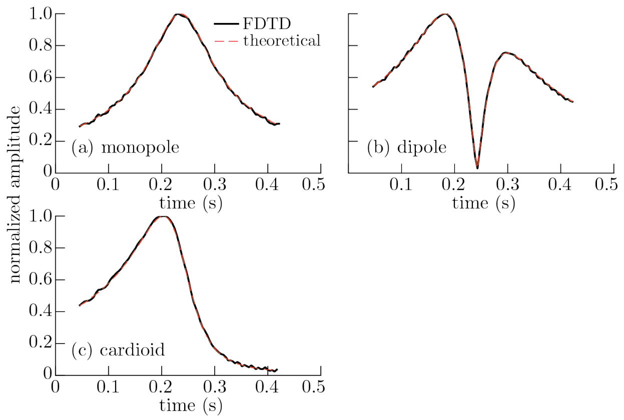

Fig.6 Normalized amplitude of a linearly passing source (M=0.1).

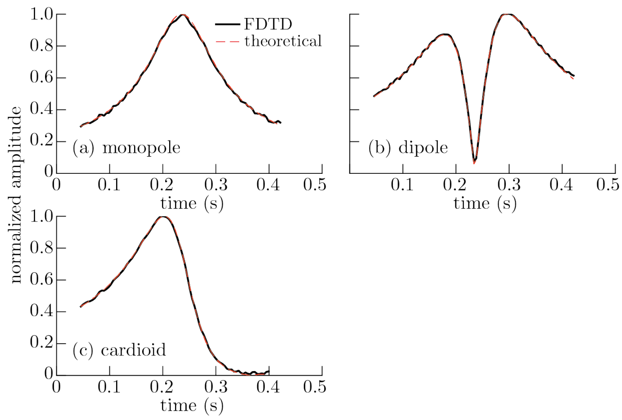

Fig.7 Normalized amplitude of a linearly passing receiver (M=0.1).

sound source and is a source when P is a receiver. The source radiates a continuous sine wave with a frequency of 500 Hz.

Figure 3 shows the directivity for the fixed source and receiver. The solid line indicates the result by FDTD method, and the red broken line is the theoretical. The calculation results and theoretical are in good agreement.

Figure 4 shows the directivity when the source moves with the speed $M = 0.1$ in the x-direction. To calculate the directivity, the receiver is also moved in the x-direction at the same speed as the source in fig. 2. The amplitude slightly increases in the moving direction. It is found that the directivity changes with the source speed as predicted by eqs. (5) and (6).

Next, the moving sound source or receiver passing linearly in front of the receiver or source is demonstrated. Figure 5 shows the numerical model for the linearly passing source or receiver. The sound source or receiver P passes linearly 2 m in front of the receiver or source Q with a constant speed of M = 0.1. Figures 6 and 7 show the normalized amplitude of the linearly passing source or receiver. In the case of moving dipole, it is evident that the amplitude is larger when the sound source is approaching and smaller when it is moving away. In the case of moving receiver, the characteristics are reversed even though the moving speed has no effect on directivity. This is because the received signal of dipole is numerically integrated, and the theoretical result has been corrected for this reason.

References

1. K. S. Yee, IEEE Trans. on Antennas and Prop., **14**, (1966) 302.
2. T. Tsuchiya et al.: Acoust. Soc. Tech., **43** (2022) 57.
3. T. Tsuchiya et al.: Jpn. J. Appl. Phys., **61** (2022) SG1036.
4. P. M. Morse and K. U. Ingard: Theoretical Acoustics, McGraw-Hill (1968).
5. K. Kowalczyk et al.: IEEE Trans. Audio Speech and Lang. Process., **18** (2010) 78.
6. T. Ishii, et al.: Jpn. J. Appl. Phys., **52** (2013) 07HC11.